Stability of the Full Spectrum Nonlinear Fourier Transform

Benedikt Leible, Daniel Plabst, Norbert Hanik
Technical University of Munich, Theresienstr. 90, 80333 Munich, Germany
e-mail: benedikt.leible@tum.de

ABSTRACT

With the seemingly inevitable "capacity crunch" for state-of-the-art fiber optical systems, alternatives to wavelength-division-multiplexing are widely discussed in the community. Recently, modulation schemes based on the nonlinear Fourier transform have been proposed, where the transmit signal is generated by modulating both the continuous and discrete nonlinear spectrum. This full spectrum nonlinear Fourier transform algorithm and its inverse are investigated and existing methods are extended to modulation of the entire nonlinear spectrum.

Keywords: fiber optical communication, nonlinear fourier transform, inverse scattering, numerical stability, algorithms

1. INTRODUCTION

In state-of-the-art high data-rate optical transmission systems, the achievable rates for high input-powers are limited, due to interactions caused by the Kerr-nonlinearity of optical fibers [1]. With the ever increasing demand for higher data rates, solutions must be provided for the estimated increase of data rates in the future. The capacity of the optical fiber channel is still an open problem and raises the question, if the Kerr-nonlinearity limit in the high input power regime is inherent to the transmission medium or if it could be overcome by a departure from state-of-the-art *linear* transmission schemes. This question leads to a variety of research trying to increase the spectral efficiency of fiber-optic communication systems using new approaches for modulation. Many publications present nonlinear frequency division multiplexing (NFDM) systems as a promising candidate for such a change [2], [3].

The nonlinear Fourier transform (NFT) transforms a time domain signal to the nonlinear Fourier domain. This is beneficial for transmission over an ideal fiber-optic channel, as the signal components propagate independently for each nonlinear frequency in the nonlinear Fourier domain. Numerical stability of NFT algorithms is still an ongoing problem in NFDM systems, especially if the entire nonlinear spectrum is used for data-transmission. Numerical instabilities restrict the usable range of the modulated parameters and thus the choice of transmission pulses for the respective NFDM systems.

In this paper, we give a short overview of the NFT, including a full spectrum implementation of the NFT algorithm and its inverse. An optimized full spectrum NFT based on [4] is presented and compared to a state-of-the-art search-based method in a back-to-back scenario.

2. THE NONLINEAR FOURIER TRANSFORM

The NFT is a transform, that represents a time domain signal by its corresponding *continuous* and *discrete* nonlinear Fourier spectrum. The NFT is derived for a loss-less, and noise-less fiber-optic channel governed by the nonlinear Schrödinger equation (NLSE). The normalized NLSE, derived in [3], is used throughout this publication:

$$\frac{\partial q(t,z)}{\partial z} = \mathrm{j}\frac{\partial^2 q(t,z)}{\partial t^2} + \mathrm{j}2|q(t,z)|^2 q(t,z), \tag{1}$$

where j is the imaginary unit and $q(t,z)$, t and z are the normalized signal, normalized time and normalized propagation distance, respectively.

The NFT generates the nonlinear Fourier spectrum of a time domain signal, supported on the *nonlinear frequencies* $\lambda \in \mathbb{C}$. The spectrum is commonly divided into two parts, the continuous and discrete spectrum, depending on the subset of λ, which they are supported on. The continuous spectrum is supported only on real-valued nonlinear frequencies and the discrete spectrum is defined only for a finite number of K complex nonlinear frequencies with a positive imaginary part ($\lambda_k \in \mathbb{C}^+$), which are called discrete eigenvalues.

Acknowledgements: This work was supported by the German Research Foundation (DFG) grant No. 320729232 "Fiber-Optic Communication via the Nonlinear Fourier Transform".

The nonlinear spectra read

$$q_{\mathrm{c}}(\lambda) = \frac{b(\lambda)}{a(\lambda)},\ \lambda \in \mathbb{R}; \quad q_{\mathrm{d}}(\lambda_k) = \frac{b(\lambda_k)}{a'(\lambda_k)},\ \text{with } a'(\lambda) = \frac{\mathrm{d}a(\lambda)}{\mathrm{d}\lambda}, \tag{2}$$

where $q_{\mathrm{c}}(\lambda)$ and $q_{\mathrm{d}}(\lambda_k)$ denote the continuous and discrete spectrum, respectively, and $a(\lambda)$ and $b(\lambda)$ are called the *nonlinear Fourier coefficients*. Details on the calculation of the nonlinear Fourier coefficients and further information on the NFT can be found in [3].

Representing a time domain signal $q(t, z)$ in the nonlinear Fourier domain results in a simple input-output relationship when the signal propagates over an *ideal* fiber-optic channel, as the nonlinear frequencies λ do not change during propagation and the spectral amplitudes $q_{\mathrm{c}}(\lambda)$ and $q_{\mathrm{d}}(\lambda_k)$ propagate independently for each nonlinear frequency λ, according to the multiplicative relations [3],

$$\frac{q_{\mathrm{c}}(\lambda, z)}{q_{\mathrm{c}}(\lambda, 0)} = \mathrm{e}^{4\mathrm{j}\lambda^2 z}, \quad \frac{q_{\mathrm{d}}(\lambda_k, z)}{q_{\mathrm{d}}(\lambda_k, 0)} = \mathrm{e}^{4\mathrm{j}\lambda_k^2 z}. \tag{3}$$

3. JOINT NONLINEAR SPECTRUM MODULATION

For the inverse nonlinear Fourier transform (INFT) of either purely continuous or purely discrete nonlinear spectra, several algorithms are already well known [5], [6] and results for the joint INFT were recently published in [7] and [8]. Figure 1 schematically shows the joint INFT, where both nonlinear spectra are modulated. First the continuous part $q_{\mathrm{c}}(\lambda)$ is used to generate a time domain seed pulse

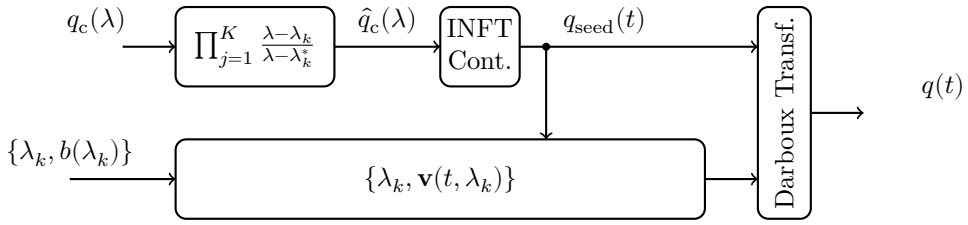

Fig. 1: Block diagram of joint spectrum modulation (based on [8])

$q_{\mathrm{seed}}(t)$, containing only continuous spectral components. This can be achieved by any of the known algorithms for the purely continuous INFT [3], [6]. Even though, no direct modifications of the continuous INFT algorithms are necessary for the algorithm in Figure 1, it needs to be considered that the continuous spectrum of a pulse changes according to [5],

$$q_{\mathrm{c}}(\lambda; \lambda_0) = \frac{\lambda - \lambda_0^*}{\lambda - \lambda_0} q_{\mathrm{c}}(\lambda), \tag{4}$$

when a discrete eigenvalue λ_0 is added to the time domain pulse $q_{\mathrm{seed}}(t)$. To this end, we pre-distort the continuous spectrum by using the inverse relationship of (4) for all K discrete eigenvalues, i.e., $\forall \lambda_k$ and $k \in \{1, \dots, K\}$, as depicted in the upper branch of Figure 1.

The time domain signal $q_{\mathrm{seed}}(t)$ is used as an initial solution, to which discrete eigenvalues are added by the subsequent Darboux transform (DT). For the discrete spectral amplitudes a relation similar to equation (4) exists [5]. To avoid using a pre-distortion similar to the one used for the continuous spectrum, instead of the corresponding spectral amplitudes $q_{\mathrm{d}}(\lambda_k)$, discrete b-values $b(\lambda_k)$ are directly modulated, because they are not affected by subsequent modification steps.

The DT is used to iteratively add eigenvalues λ_k and their corresponding nonlinear coefficients $b(\lambda_k)$ to the discrete spectrum of $q_{\mathrm{seed}}(t)$ [3], [5]. To facilitate this, the Jost solutions of the Zakharov-Shabat (ZS) system $\mathbf{v}(t, \lambda_k)$ have to be computed for the boundary conditions given in [3]. In theory this can be done by using any numerical integration method, but to mitigate numerical issues the *forward-backward* method [8] is used.

After the Jost solutions are computed for $q_{\mathrm{seed}}(t)$ the DT can be used to add the discrete nonlinear spectrum to the pulse, finally generating the transmission pulse $q(t)$ containing the modulated continuous and discrete nonlinear spectra.

4. EIGENVALUE REMOVAL NFT

To increase the reliability at the detection side, a recently presented modification of the NFT is used [4]. The algorithm iteratively detects discrete eigenvalues and removes them from the received pulse. While in [4] the algorithm was only used for a purely discrete spectrum, i.e., solitonic pulses, it can also be used to aid in the retrieval of both spectra.

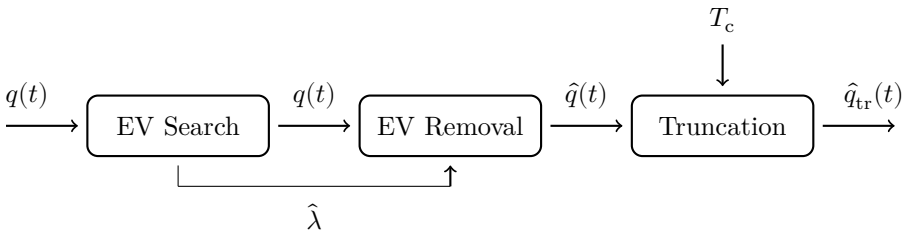

Fig. 2: Block diagram of one eigenvalue removal step.

The steps for removing one eigenvalue are depicted in Figure 2. Initially a search in $q(t)$ for the discrete eigenvalue $\hat{\lambda}$ with the smallest imaginary part is run. Subsequently the eigenvalue is removed by using [4]

$$\hat{q}(t) = q(t) + \frac{2\mathrm{j}(\hat{\lambda}^* - \hat{\lambda}) v_2^*(t,\hat{\lambda}) v_1(t,\hat{\lambda})}{|v_1(t,\hat{\lambda})|^2 + |v_2(t,\hat{\lambda})|^2}, \tag{5}$$

where $q(t)$ and $\hat{q}(t)$ are the time domain pulses before and after the removal of $\hat{\lambda}$, respectively. The Jost solutions $\mathbf{v}(t,\hat{\lambda}) = \left[v_1(t,\hat{\lambda}), v_2(t,\hat{\lambda})\right]$ have to be obtained beforehand from $q(t)$, which can be done similarly to the process explained in Section 3. For successful removal, it is necessary to have a fairly good estimate for $\hat{\lambda}$. If the estimate deviates too much from the true value, an additional eigenvalue is added to the pulse. The energy of the resulting pulse $\hat{q}(t)$ can be used to monitor the success of every removal step.

After removal of an eigenvalue, the time-domain support of the pulse is truncated, since it can be assumed that the pulse-width decreased if the time duration of $q_\mathrm{seed}(t)$ is smaller than the duration of $q(t)$. The truncated pulse $\hat{q}_\mathrm{tr}(t)$ is then used as an input for the next eigenvalue removal step. The truncation of the time-domain support of the pulse results in an improvement of the numerical estimation error, which is beneficial for the next eigenvalue search [4, P. 3]. Furthermore, the computational complexity is reduced for the following searches, as the number of samples has effectively been reduced.

Eigenvalues resulting in time domain pulse contributions with high amplitude and small time duration, focus most of the energy of the pulse at its center. Thus, if the signal parts corresponding to the continuous spectrum are broader in time, they are subjected to larger truncations if the energy contribution of the continuous spectral part is smaller than the contribution of the discrete spectral part. Thus, a minimal duration T_c is introduced to guard the continuous part of the spectrum. The steps depicted in Figure 2 are repeated until all eigenvalues are found and removed. The resulting impulse should now only contain the continuous spectrum and can be detected with any standard NFT. Note that by successful removal of an eigenvalue, the continuous spectrum is altered according to the inverse of (4), which has to be taken into account.

5. SIMULATION RESULTS

Simulations testing the INFT/NFT configuration in a back-to-back setup are conducted for symbols with $N = 2^{10}$ samples. The symbols are generated from their respective nonlinear Fourier spectra using the algorithm from Section 3. The continuous nonlinear spectrum consists of a single channel with a root raised cosine (RRC) shape and amplitude A in frequency domain, which is modulated by a random symbol drawn from a unit power PSK constellation, with uniform independently and identically distributed (iid) phase $\phi \in [0, 2\pi)$.

The nonlinear Fourier coefficient $b(\lambda_k)$ for the two discrete eigenvalues $\lambda_1 = \mathrm{j}\kappa,\ \lambda_2 = \mathrm{j}2\kappa$ is modulated, and the parameter κ is varied during simulations. The values for $b(\lambda_k)$ are also randomly drawn from a phase shift keying (PSK) constellation with unit power and uniform iid phase $\phi \in [0, 2\pi)$.

The continuous INFT is implemented by the discrete layer peeling (DLP) method [6]. The trapezoidal forward-backward method [5], using a search based scheme for the discrete part, is used as a state-of-the-art NFT for comparison with the eigenvalue removal method described in Section 4. For each data point $N_\mathrm{r} = 2048$ pulses are generated by the INFT and detected by the two NFTs. The results are depicted in 3. As it can be seen in Fig. 3a the factor $\delta_\mathrm{e} = \frac{\mathrm{NMSE_r}}{\mathrm{NMSE_s}}$ between the normalized mean square error (NMSE) of the eigenvalue removal method $\mathrm{NMSE_r}$ and the NMSE of the search based method $\mathrm{NMSE_s}$ is nearly constant over all tested value pairs. Hence both methods before equally well for the continuous spectrum, whereas the proposed method is cheaper from a computational complexity point of view. For the discrete eigenvalues and the modulated b-values in Figures 3b and 3c, it can be seen that the detection error can

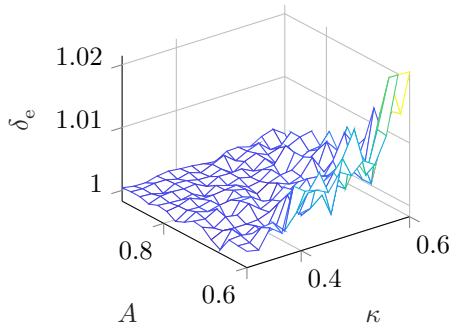

(a) Continuous spectrum NMSE quotient δ_e.

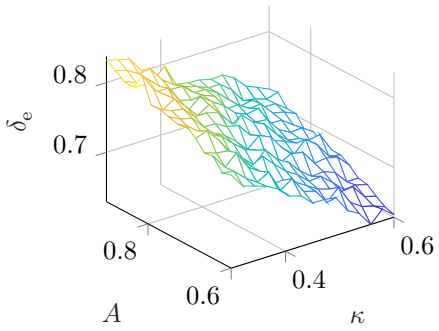

(b) Discrete eigenvalues NMSE quotient δ_e.

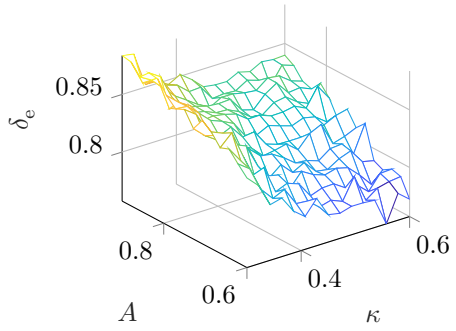

(c) Discrete b-values NMSE quotient δ_e.

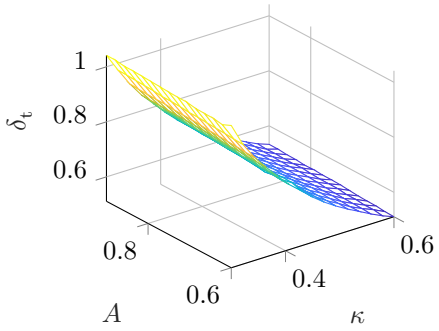

(d) Computation time quotient.

Fig. 3: Comparison of detection algorithms for $K = 2$ eigenvalues δ_e.

be reduced by a factor of nearly 40% for discrete eigenvalues with larger imaginary parts. The change to a constant slope $\mathrm{d}\delta_e/\mathrm{d}\kappa$ in Fig. 3c for larger κ can probably be attributed to the fixed truncation guard interval T_c. Finally the factor δ_t, by which the computation time is reduced using the removal method instead of the search based NFT, is given in 3d. Again, for larger values of κ, the time for computation can be reduced by nearly 50%, saturating for larger κ, presumably due to the same reasons as for the slope $\mathrm{d}\delta_e/\mathrm{d}\kappa$.

6. CONCLUSION

One major issue regarding NFDM based fiber-optic systems are algorithms with high computational complexity, exhibiting numerical instabilities when the modulated parameters exceed a certain range of values. To mitigate this effect and reduce the complexity of the algorithms in the receiver for modulation of the entire nonlinear spectrum, an eigenvalue removal NFT was implemented. In a simulation it was shown that this NFT performs better than state of the art search based alternatives for the majority of the tested parameters. There are many directions for future research: is could be studied if the observations regarding Fig. 3 are also visible for higher-order modulation schemes or a larger amount of discrete eigenvalues. Furthermore, it would be interesting to see how the discussed algorithms perform in a practical transmission scenario.

REFERENCES

[1] R.-J. Essiambre, G. Kramer, P. J. Winzer, G. J. Foschini, and B. Goebel, "Capacity Limits of Optical Fiber Networks," *Journal of Lightwave Technology*, vol. 28, no. 4, pp. 662–701, 2010.

[2] M. J. Ablowitz and H. Segur, *Solitons and the inverse scattering transform*. Siam, 1981, vol. 4.

[3] M. I. Yousefi and F. R. Kschischang, "Information Transmission Using the Nonlinear Fourier Transform, Part I-III," *IEEE Transactions on Information Theory*, vol. 60, no. 7, pp. 4312–4328, 2014.

[4] A. Span, V. Aref, H. Buelow, and S. t. Brink, "Successive eigenvalue removal for multi-soliton spectral amplitude estimation," *arXiv preprint arXiv:2004.02974*, 2020.

[5] V. Aref, "Control and detection of discrete spectral amplitudes in nonlinear fourier spectrum," *arXiv preprint arXiv:1605.06328*, 2016.

[6] M. Yousefi and X. Yangzhang, "Linear and nonlinear frequency-division multiplexing," *IEEE Transactions on Information Theory*, 2019.

[7] V. Aref, S. T. Le, and H. Buelow, "Demonstration of fully nonlinear spectrum modulated system in the highly nonlinear optical transmission regime," in *ECOC 2016-Post Deadline Paper; 42nd European Conference on Optical Communication*. VDE, 2016, pp. 1–3.

[8] ——, "Modulation over nonlinear fourier spectrum: Continuous and discrete spectrum," *Journal of Lightwave Technology*, vol. 36, no. 6, pp. 1289–1295, 2018.